PROCEEDINGS, 49th Workshop on Geothermal Reservoir Engineering
Stanford University, Stanford, California, February 12-14, 2024
SGP-TR-227

Fluid Flow and Thermal Anomalies in Naturally Fractured Media: A new Guide for Geothermal Exploration of Crustal Fault Zone

Hugo Duwiquet*, Albert Genter[1], Laurent Guillou-Frottier[2,3], Frédéric Victor Donzé[4], Patrick Ledru[5], Fabien Magri[6,7], Théophile Guillon[2], Roland H. Horne[8], Laurent Arbaret[3], Christine Souque[9]

[1]ES-Géothermie, 26, Boulevard du Président Wilson, 67000, Strasbourg, France. [2]BRGM, 3 Av. C. Guillemin, BP 36009, 45060, Orléans Cedex 2, France. [3]Univ. Orléans, CNRS, BRGM, ISTO, UMR7327, 45071, Orléans, France. [4]Université Grenoble Alpes, Université Savoir Mont Blanc, CNRS, IRD, IFSTTAR, ISTerre, 38000 Grenoble, France. [5]Université Lorraine, UMR 7359 GeoRessources, 54506 Vandoeuvre les Nancy, France. [6]Division Research/International, BASE, The Federal Office for the Safety of Nuclear Waste Management, Berlin, Germany. [7]Institut of Geological Sciences, Hydrogeology Group, Freie Universität Berlin, Berlin, Germany. [8]Department of Energy Resources Engineering, Stanford University, Stanford, CA 94305. [9]IFP Energies nouvelles, 1-4 avenue Bois-Préau, 92852 Rueil-Malmaison, France.

*hugo.duwiquet@engie.com

Keywords: Geothermal exploration, Multiphysics Modeling

ABSTRACT

In context of global change, Crustal Fault Zones emerge as intriguing geological prospect for geothermal energy resources in naturally deep fractured basements. The occurrence of a positive temperature anomaly is conditioned upon an array of geological and physical parameters. The goal of this study is to proffer a non-exhaustive inventory of some of these parameters: thickness of the fault zone, dip of the fault zone, permeability and tectonic regimes. By employing 2D and 3D numerical modeling, with TH and THM couplings, we can discern different favorable criteria that may serve as guiding exploration: (i) thermal convection is more vigorous where the fault zone thickness is largest, (ii) strike-slip systems foster the extension of positive temperature anomalies, and (iii) vertical and subvertical fault zones concentrate the highest temperature anomalies at shallow depths. Consequently, the identification of these new favorability criteria paves the way for the selection of other fault zones as potential targets for geothermal energy, as it was recently done in Western Europe.

1. INTRODUCTION

Dating back to the initiation of inaugural electricity production in Larderello, Tuscany (20 kW in 1905), geothermal energy has undergone extensive global development. In 2023, the foremost five contributing nations include the USA (3,900 MW), Indonesia (2,418 MW), Philippines (1,952 MW), Turkey (1,691 MW), and New Zealand (1,042 MW) (www.thinkgeoenergy.com). Globally, the installed capacity for electricity generation stands at 16 GWe, corresponding to an annual output of 95 GWh (Huttrer, 2020; Lund et al., 2020). This production hinges on the geological paradigm of geothermal reservoirs, emphasizing the imperative of a heat source, fluid, and adequate permeability to facilitate fluid flow. This present-day geological model of geothermal reservoirs leads exploration endeavors toward distinct and well-established geodynamic and tectonic systems, such as magmatic arcs, subduction zones, pull-apart basins, and extensional and crustal thinning systems (Moeck, 2014; Jolie et al., 2021). Nevertheless, in purely basement systems and devoid of an additional heat source, anomalously permeable zones, such as crustal fault zones, should exhibit all the requisite physical characteristics for the manifestation of a temperature anomaly at economically viable depths. The identification of potential new targets may lay the groundwork for the accelerated development of geothermal energy.

In the crustal domain, fault zones constitute intricate volumes of fractured and deformed rocks with varying geometries, evolving across three spatial dimensions and one temporal dimension (Wibberley et al., 2008). Within the Earth's crust, these zones localize deformation (Ben-Zion and Rovelli, 2014) and modify crustal properties above the brittle-ductile transition. Field observations indicate lateral facies variations among damaged, crystallized, and undeformed zones, resulting in noteworthy permeability fluctuations within these fault zones (Faulkner et al., 2003). Estimated to exceed 500 globally (Scibek, 2020), these potential targets, with their diverse geometries and physical parameters, underscore the variability in geological and physical attributes that could either facilitate or impede the occurrence of positive temperature anomalies.

In 1778, de Buffon stood among the pioneers in postulating that fluids, heated by the Earth's internal warmth, could permeate through what were then denoted as 'rock crevices.' Within crustal domains marked by anomalously elevated permeability, such as fault zones, vertical thermal instabilities might be intricately linked with fluid dynamics within convective cells (Caltagirone, 1975; Horne, 1979; Murphy, 1979; López and Smith, 1995; Faulds et al., 2010; Magri et al., 2016). Diverse parameters exert influence over the dynamics of convective cell. Fluid properties such as viscosity and density, alongside the permeability ratio between the fault and the basement (López

and Smith, 1995), stand as recognized variables that affect fluid flow and heat transfer. Nevertheless, an array of other geological and physical parameters, acknowledged for their inherent variability, may or may not contribute to the manifestation of a temperature anomaly.

For fault zones, the geometric (G) position in space is defined by a set of constants including thickness. In 1875, in Colorado (USA), J. W. Powell observed varying thicknesses within a single fault zone. This included a thin deformation zone (several centimeters) without notable filling and a thicker deformation zone (several tens of meters) characterized by block filling. The dip of the structures is also a variable geological parameter. Numerous studies have defined hydrothermal systems embedded within fault zone exhibiting dips of 30°, 60° and 90° (Faulkner et al., 2003; Wisian and Blackwell, 2004; Famin et al., 2004). Furthermore, stress orientation and more broadly tectonic regimes have been recognized both as significantly variable parameters, and as driving force influencing fluid flow in various geological contexts (Ord and Oliver, 1997; Rowland and Sibson, 2004).

Employing a dynamic numerical modeling approach, this study investigates the influence of a non-exhaustive list of geological and physical parameters on fluid flow within anomalously permeable zones of the Earth's crust. The study does not account for the effects of fluid geochemistry and topography. Nevertheless, it does delve into the impacts of 3D fault zone thickness variability, tectonic regimes, and dip concerning convective dynamics and temperature distribution. Through the systematic testing of various parameter ranges, our objective is to identify trends that not only demonstrate the predictive capabilities of numerical modeling but also have the potential to influence exploration campaigns and drilling strategies.

2. METHODOLOGY

To assess the distinct influence of variations in thickness, fault dip, and tectonic regimes on fluid flow and thermal distribution, a series of numerical simulations were conducted. Employing the Finite Element Method (FEM), the Comsol Multiphysics™ software facilitates the integration of diverse time-dependent physical phenomena, including fluid dynamics, heat transfer, and elastic deformation of materials, within both 2D and 3D geometries. For different coupling we applied Darcy's law, Fourier's law, and Hooke's law in our numerical experiments. The model configuration, specifics of the coupling, and the equations utilized are comprehensively outlined in Duwiquet et al. (2019), Guillou-Frottier et al. (2020), Duwiquet et al. (2021a), and Duwiquet et al. (2022).

To investigate the specific influence of tectonic regimes on fluid flow, we used the Andersonian assumption, which is regularly used in geomechanical reservoir studies (Zoback et al. 2003). The principal stresses are expressed with vertical (Sv), maximum horizontal (SHmax), and minimum horizontal (Shmin) components. Note that the relative stress magnitude determine the modeled tectonic regime:

Compressional (reverse/thrust faulting), with SHmax ≥ Shmin ≥ Sv

Extensional (normal faulting), with Sv ≥ SHmax ≥ Shmin

Strike-slip, with SHmax ≥ Sv ≥ Shmin

As the model is aligned with the principal stresses, pure normal stresses are applied on the lateral boundaries. For the compressional tectonic regime, the fault is perpendicular to the SHmax stress while for the extensional tectonic regime, the fault is perpendicular to Shmin. Lastly, for the strike-slip regime, the fault is at 45° between Shmin and SHmax orientation. Vertical stress Sv can be expressed as a function of the rock maximum weight forces and then adjust the horizontal/vertical stress ratios to accommodate different tectonic regimes:

$$\begin{cases} S_{\mathrm{V}} = \rho_{\mathrm{s}} \times g \times (-z) \\ S_{\mathrm{Hmax}} = \alpha_{\mathrm{Hmax}} \times S_V \\ S_{\mathrm{hmin}} = \alpha_{\mathrm{hmin}} \times S_V \end{cases} \quad (1)$$

where ρ_{s} [kg. m^{-3}] is the rock mass density (see Table 1), g [$m^2.s^{-1}$] is the gravity acceleration, and z [m] is the vertical upwards axis. An increase in depth ($z < 0$) results in more compressive stress (positive compression convention). α_{Hmax} [$-$] and α_{hmin} [$-$] are the horizontal-to-vertical stress ratios. To accommodate different tectonic regimes, we must set:

- compressional: $\alpha_{\mathrm{Hmax}} \geq \alpha_{\mathrm{hmin}} \geq 1$
- extensional: $1 \geq \alpha_{\mathrm{Hmax}} \geq \alpha_{\mathrm{hmin}}$
- strike-slip: $\alpha_{\mathrm{Hmax}} \geq 1 \geq \alpha_{\mathrm{hmin}}$

The values for the stress ratios remain to be estimated. A comprehensive parametric study would require testing various values for each tectonic regime. However, to follow a step-by-step approach and limit the number of unknowns, we decided to fix these values based on literature data. The San Andreas stress regime was chosen as it is a well-documented system and results in a highly deviatoric configuration, thus intensifying the stress effects (Zoback, 1992).

3. RESULTS

3.1 Influence of fault Zone thickness variability on fluid flow dynamics

3.1.1 Critical Rayleigh number analysis

In order to investigate the initiation of thermal convection within a permeable faulted zone of limited width, Malkovsky and Magri (2016) conducted a linear stability analysis. Their study represents an improvement over the earlier work by Malkovsky and Pek (1997), which assumed a constant viscosity. The fault zone is characterized by a half-thickness δ and a height H, and the fluid viscosity varies with temperature. They demonstrated that the critical Rayleigh number can be expressed as:

$$Ra^{crit} = a \times \left[\left(\frac{8.19 \times H}{\delta} \right)^{5/4} + (4\pi^2)^{5/4} \right]^{4/5} \quad (2)$$

where a is a constant equal to 1 for the case of constant viscosity and 2.466 for the case of temperature-dependent viscosity with an average temperature gradient (see Malkovsky & Magri, 2016). In the scenario of an infinitely wide fault with constant viscosity, the value of $4\pi^2$ (Lapwood, 1948) is obtained. Figure 1 illustrates the influence of fault width on the critical Rayleigh number for various fault heights. In wider fault zones (ranging from hundreds to thousands of meters), the critical Rayleigh number decreases by 1 to 2 orders of magnitude compared to fault widths in the tens of meters, facilitating thermal convection.

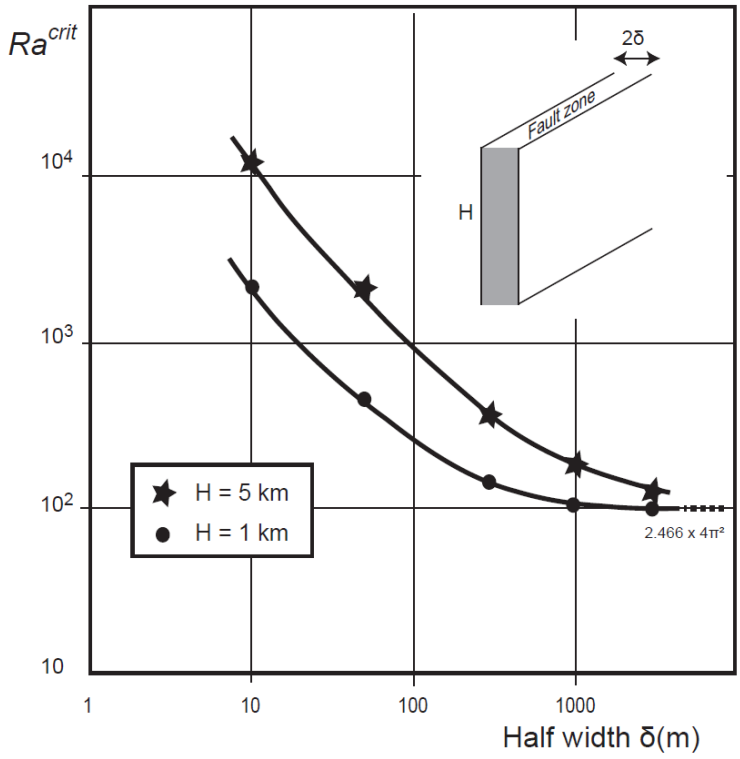

Figure 1: Graph depicting the relationship between the critical Rayleigh number and fault width for three distinct fault heights derived from the theoretical analysis conducted by Malkovsky and Magri (2016). Duwiquet et al., submitted.

The analysis of the critical Rayleigh number reveals that the thickness of the fault zone significantly influences fluid flow dynamics. Therefore, we propose to investigate these effects through 3D dynamic numerical experiment.

3.2 3D TH numerical modeling

In its 3D geometry, the model includes on the upper horizontal part, the pressure is 10^5 Pa, and the temperature is 10 °C. At the bottom part of the model, a heat flux of 100 mW/m^2 is imposed. The vertical faces of the crust are thermally insulated and fluid flow is blocked. The preliminary results from the 3D numerical experiment are presented in steady-state and indicate that fluid circulation occurs on both sides of the fault (Figure 2). As its density increases due to the cooling effects of the top boundary condition, the fluid sinks within the fault volume, leading to a classic natural convection pattern related to buoyancy forces. Under these conditions, this free convection generates a thermal disturbance. In a purely diffusive setting, the 150°C isotherm is observed at a depth of 5 km, whereas, in the area with the thickest deformation zone, the same isotherm is found at a depth of 2.7 km (Figure 2). In the thinnest zone, the 150°C isotherm

rises to a depth of 3.3 km. In the thickest part of the fault, fluid flow is defined by a vigorous convective cell (Figure 2). It is established along the X and Y axes and is characterized by both downward and upward motions. The wavelength of the convective cell occupies only one-third of the fault surface area. Fluid velocities vary between 1×10^{-9} m/s and 16×10^{-9} m/s. The lowest velocities are concentrated in the bottom part of the convective cell, while the highest velocities are concentrated in the top part of the convective cell. In the thinnest part of the fault, fluid flow is also present, but fluid velocity values are much lower and the consequent thermal anomaly is weak(Figure 2).

Less vigorous, the fluid upwelling is barely visible at the bottom of the fault. The upwelling of the isotherms is more indicative of this convection, which, while less strong, has a significant wavelength, as it occupies two-thirds of the fault surface area. In line with the critical Rayleigh number analysis (Figure 1), our preliminary 3D dynamic numerical results reveal that thermal convection is more efficient in areas where the fault thickness is thickest. Arising from a theoretical and simplified investigation, this initial discerned trend must be validated through more comprehensive and data-constrained fault zone, where thickness variations have been identified (e.g the Carboneras Fault Zone (Andalusia, Spain), Faulkner et al., (2003)).

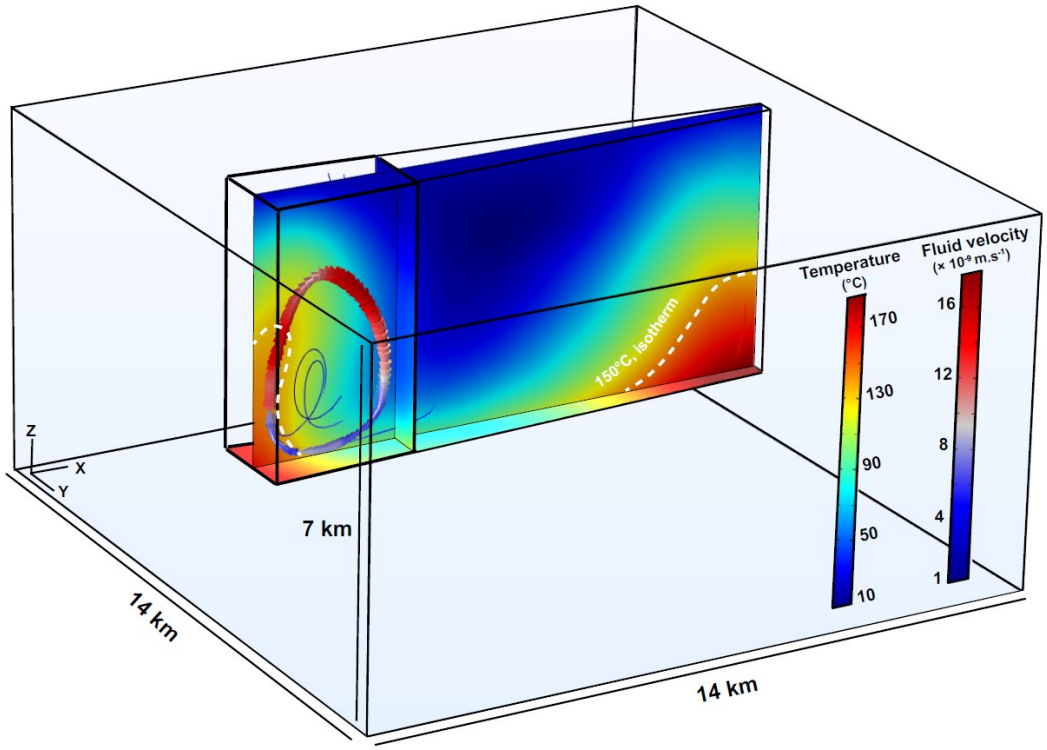

Figure 2: Preliminary 3D numerical modeling of a fault zone of varying thickness. The results is given in steady-states condition. The temperature distribution is visualized using a color scheme, where the highest temperatures are depicted in red and the lowest temperatures in blue. Fluid flow is indicated by lines, with arrows denoting the direction of circulation. Fluid velocities are illustrated, with red representing the highest velocities and blue representing the lowest. (Duwiquet et al., submitted)

3.3 Exploring the influence of diverse tectonic regimes on fluid flow within fault zones

Regardless of the considered tectonic regime (for more details on boundary conditions see Duwiquet et al., 2022), positive and negative temperature anomalies are observed (Figure 3). They differ by their number, intensity and lateral extension (Figure 3). In extensional tectonic regime, two positive temperature anomalies are found. The highest is +55°C and the lowest is +10°C. A negative temperature anomaly of -60°C is localized at the center of the fault. At 2 km depth, the horizontal cross-section shows a negative temperature anomaly that reaches a maximum of -30°C. This anomaly covers a large surface area of the fault. The positive temperature anomaly of +45 °C occupies the remaining space, but extends further into the basement. In the basement and up to the edge of the model, we find a positive temperature anomaly of +20°C. The fluid flow pattern is characterized by a downward movement at the center of the fault and two upward movements at the ends of the fault. The minimum fluid velocity is 5×10^{-9} m.s^{-1} and the maximum is 30×10^{-9} m.s^{-1}. In compressional tectonic regime, we find two positive temperature anomalies. The value of the maximum temperature anomaly is +60°C. The second temperature anomaly is +40°C. In horizontal cross-section, the values of these two temperatures anomalies are +56 and +47°C, respectively. The lateral extension of these temperature anomalies is limited. They are surrounded by negative temperature anomalies that locally reach -47°C. At a depth of 2 km, the positive temperature anomalies are much less extended than in extensional tectonic or strike-

slip regimes (see below). There are two upward and two downward movements. The minimum fluid velocity is 1×10^{-9} m.s^{-1} and the maximum is 5×10^{-9} m.s^{-1}.

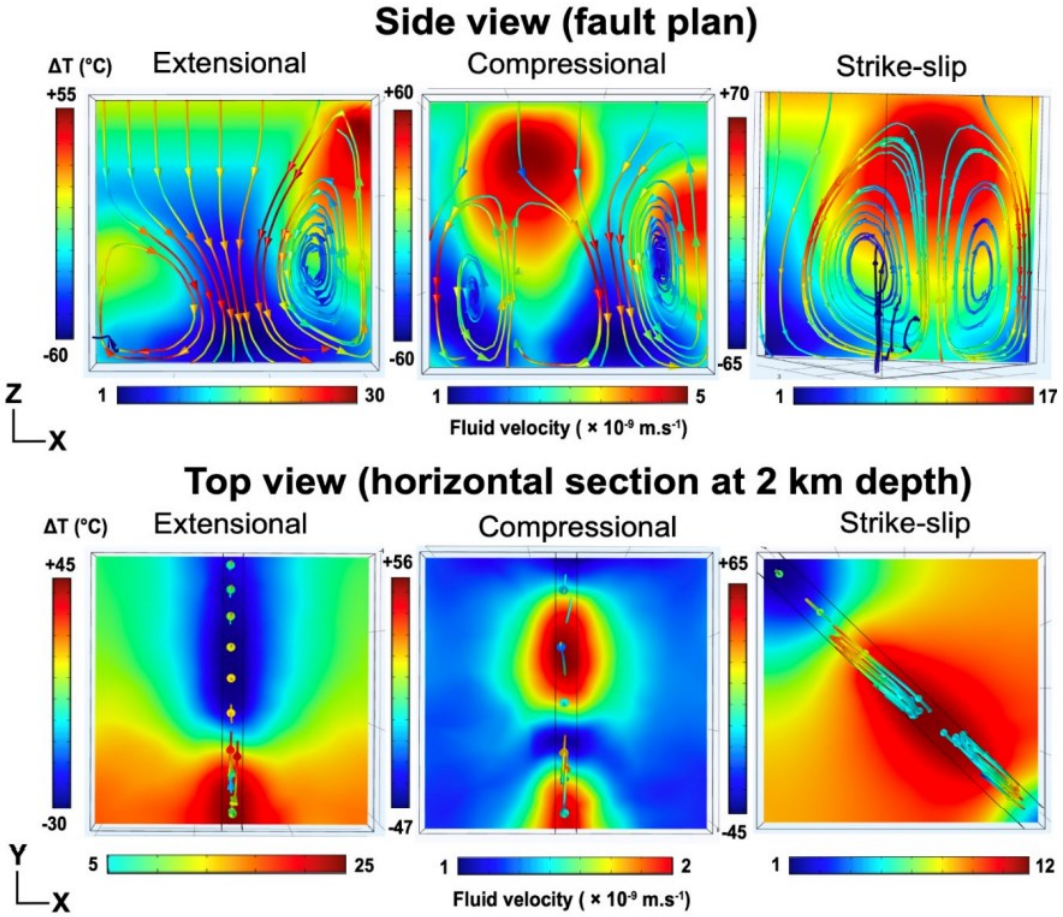

Figure 3: The numerical modeling results following the application of stresses are presented (for more detailed, refer to Duwiquet, 2022). The results are displayed in both a vertical section (Side view) located at the center of the fault and a horizontal section (Top view) positioned at a depth of 2 km. The scale of temperature anomalies and fluid flow velocities varies based on the specific tectonic regimes. For each regime, the maximum and minimum values of temperatures and fluid flow velocities are indicated. Positive temperature anomalies are represented by the color red, while negative temperature anomalies are depicted in blue. Fluid flow is illustrated by lines, with arrow heads indicating the direction. The color of the lines corresponds to the fluid velocity, with red representing the highest velocity and blue indicating the lowest velocity.

In strike-slip regimes, positive temperature anomaly extends widely along the length of the fault, from the surface to 4.5 km deep (Figure 3). The maximum positive temperature anomaly value is +70°C. Temperature anomalies of 25°C are found in the basement suggesting that, for strike-slip system, the positive temperature anomaly represents a large volume. This heat propagation is achieved by thermal diffusion from the fault center, where the temperature anomaly is highest. Indeed, the larger the convection cell inside the fault, the wider the extent of the diffusive perturbation. At 2 km depth, the maximum value of the temperature anomaly is +65°C. Negative temperature anomalies are present and localized at the extremities of the fault. The fluid flow pattern is characterized by an upward movement at the center of the fault and two downward movements at the ends of the fault. In strike-slip regime, the temperature anomaly extends largely in the basement. This is not the case for the other tectonic regimes tested. The minimum fluid velocity is 1×10^{-9} m.s^{-1} and the maximum is 17×10^{-9} m.s^{-1}.

Tectonic regimes influence the distribution and the amplitude of temperature anomalies (Figure 3). Positive temperature anomalies are most intense in strike-slip, then in compression and extension. The spatial extent of positive temperature anomalies is not identical for each tectonic regime. In strike-slip, these anomalies are largely extended through the basement. This lateral extension is less pronounced in the extensive tectonic regime. Finally, in a compressional regime, these anomalies are localized in the near vicinity of the fault. The tectonic regimes have a key role in the temperature distribution, and this is clearly related to the different convective patterns and fluid

flow velocity, as described below. In reply to the application of different tectonic regimes, the fluid pressure for each tectonic regime is different. The convection is not only linked to buoyancy forces, but also to what we call "poroelasticity driven force" and thus, the convection is here forced (for more details see Duwiquet, 2022).

3.4 Effect of fault dip on fluid flow

To assess the influence of fault dip on fluid flow, we conducted 2D simulations (Figure 4a) as well as 3D simulations (Figure 4b and c). As shown in Figure 4a, for R = 200, as the dip of the fault zone increases from 10 to 90°, the temperature values rise from 12 to 85.4 °C (indicated by red numbers). Therefore, for a fixed R ratio, the greatest thermal anomaly occurs in a vertical fault zone. The depth of the thermal anomaly also varies with fault dip. Increasing the fault dip from 10 to 90° leads to a decrease in the depth of the thermal anomaly (indicated by brown numbers), from 3.6 to 0.7 km. Consequently, for a fixed R value, vertical structures result in the largest thermal anomalies at shallower depths. The driving force behind these fluid circulations is buoyancy. However, fluid circulation can occur in three dimensions (Magri et al., 2016; Patterson et al., 2018). The trends observed in 2D could therefore be modified. In 3D, considering thermal-hydraulic coupling, Guillou-Frottier et al. (2020) investigated the influence of dip on a fixed permeability structure.

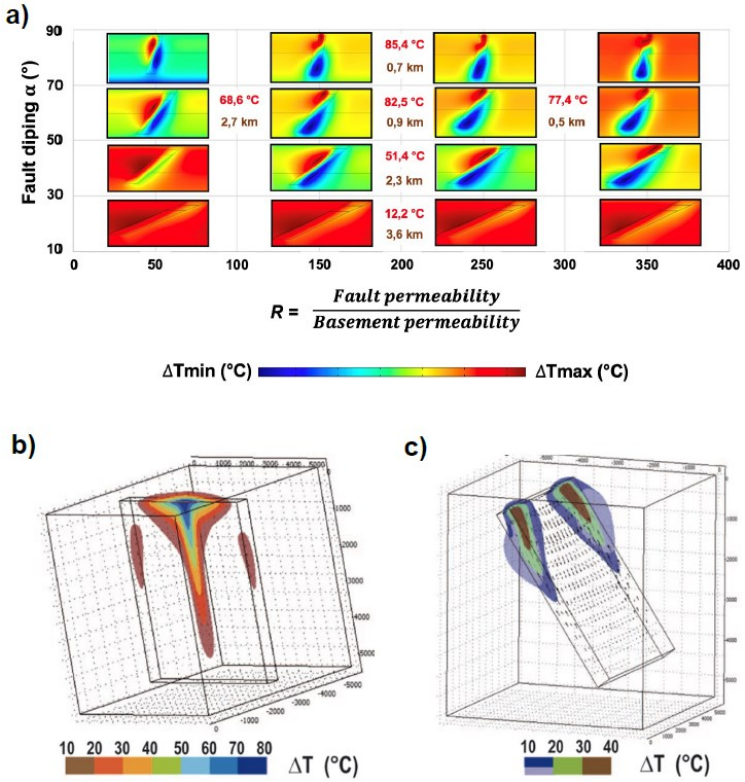

Figure 4: Results of numerical modeling in 2D a) (from Duwiquet et al., 2019) and 3D b) and c) (from Guillou-Frottier et al., 2020) with dips tested between 0 and 90°. In these different dimensions, the trends show that vertical structures concentrate the most intense positive temperature anomalies at the shallowest depths (a, b and c).

Two 3D experiments are presented, varying the angle of the permeable structure from 0 to 45°. Figure 4b and c illustrates the results of these experiments, revealing differences in the values of temperature anomalies. The vertical case yields the largest temperature anomaly. The trends observed in 2D appear to hold in 3D as well. Whether in 2D or 3D, the underlying control mechanism could be the temperature difference between the base and top of the geological structure. With a constant structure length, temperatures at the base are higher for steeper dips compared to shallower dips. This discrepancy between the base and top of the permeable structure directly influences the formation of convection cells. These preliminary 2D and 3D findings demonstrate a tendency for vertical or subvertical structures to focalize the most heightened temperature anomalies.

3. DISCUSSIONS

Numerous factors can exert influence on fluid flow within fault zones, rendering the 2D and 3D dynamics of convective pattern complex. The principal aim of this investigation is to scrutinize a comprehensive array of diverse geological and physical variables, such as thickness, tectonic regimes, and the dip of an anomalously permeable zone. A first constitutive step of this work, was to approve our numerical approach by reproducing the results of numerical modelling performed with the OpenGeoSys code (Magri et al., 2017) and Comsol Multiphysics^{TM} V3.5a (Guillou-Frottier et al. 2020). While the similarity of the results is not explained here, it is detailed in Duwiquet et al. (2022).

Lateral variation in the 3D thickness of a fault zone exerts a discernible influence on convective dynamics. In steady-state conditions, fluid flow occurs where the thickness is greatest (Figure 1, 2). Prior to juxtaposing these outcomes with those observed in natural systems, it becomes imperative to quantitatively ascertain the critical thickness at which thermal convection is predisposed to initiate. This, in turn, allows for a more precise targeting of the upward flow of fluid circulations, thereby inducing the emergence of a positive temperature anomaly, as illustrated in Figure 2. This quantitative approach was already conducted in 2D, as detailed by Guillou-Frottier et al. (2024). Within this investigation, the authors prominently emphasized that favorable conditions for the emergence of a positive temperature anomaly in naturally fractured domains would be (i) a damage zone thickness > 100 m, (ii) a minimum cumulative displacement of 100-150 m and (iii) fault zone lengths of at least one kilometer (Guillou-Frottier et al., 2024). Based on these favorability criteria, and on a large database (Scibeck, 2020), the authors propose a mapping of potential geothermal targets in Europe (Figure 5).

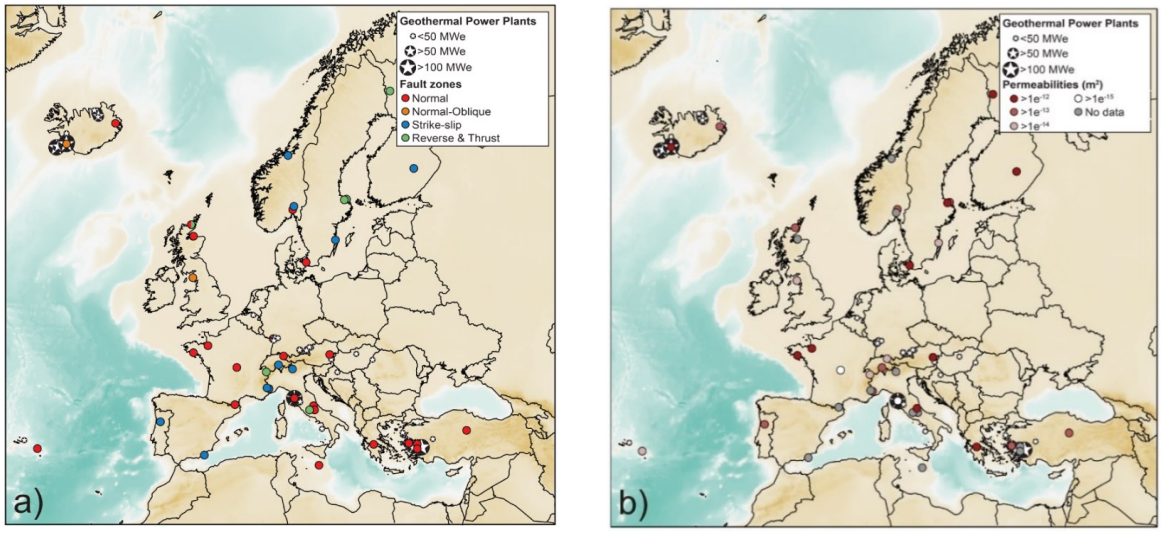

Figure 5: (a) Geothermal fields installed and exploited in Europe (https://www.thinkgeoenergy.com/map/). Selected fault zones from the database of Scibek (2020), with geometrical criteria. (b) Map showing the main faults permeabilities from the database of Scibek (2020). (For more details, see Guillou-Frottier et al. (2024)).

Other natural systems can be juxtaposed with the trends discerned in this study. For instance, the Chingshui subvertical fault zone (Ilan, Taiwan), exhibits upward fluid movements that raise isotherms facilitating exploitable opportunities, as described by Lun-Tao et al. (2008). Moreover, since the onset of 2020, the United Downs Deep Geothermal Project (UDDGP) has been attempting to target a naturally fractured reservoir within the heat producer Cornish granite (Ledingham et al., 2019, Paulilla et al., 2020). The structural verticality and the significance of the strike-slip system stand out as two favorability criteria discussed in the study (Figure 3, 4).

3. CONCLUSIONS & PERSPECTIVES

Expanding the scope of potential targets for geothermal energy entails the exploration of novel zones within the Earth's continental crust. Crustal fault zones represent abnormally permeable deep regions within the crust, enabling fluid circulation through convection without requiring an additional heat source, such as the presence of a magma chamber. Nevertheless, the heterogeneous and variable characteristics of these geological structures contribute to the high sensitivity of recorded convective patterns. The objective of this study is to present a non-exhaustive list of varied geological and physical parameters observed in natural systems. The outcomes of both 2D and 3D idealized numerical modeling, incorporating thermal-hydrologic (TH) and thermo-hydro-mechanical (THM) couplings, were employed to delineate the impact of geological and physical parameters on fluid flow. These numerical models do not consider the influence of fluid geochemistry. However, if these findings are to be utilized as a roadmap for exploration, several crucial points should be taken into consideration: (i) thermal convection exhibits greater intensity in regions with the widest fault thickness, (ii) strike-slip systems facilitate the expansion of positive temperature anomalies, and (iii) vertical and subvertical faults concentrate the most significant temperature anomalies at shallower depths."

REFERENCES

Ben-Zion, Y., & Rovelli, A.: Properties and processes of crustal fault zones: volume I. Pure and Applied Geophysics, 171, (2014), 2863-2865.

Caltagirone, J. P.: Thermoconvective instabilities in a horizontal porous layer. Journal of Fluid Mechanics, 72(2), (1975), 269-287.

de Buffon G-L (1778): Les époques de la nature. In : Histoire naturelle, vol XII. De l'imprimerie Royale, A Paris (in French).

Duwiquet, H., Arbaret, L., Guillou-Frottier, L., Heap, M. J., & Bellanger, M.: On the geothermal potential of crustal fault zones: a case study from the Pontgibaud area (French Massif Central, France). Geothermal Energy, 7, (2019), 1-29.

Duwiquet, H., Guillou-Frottier, L., Arbaret, L., Bellanger, M., Guillon, T., & Heap, M. J. (2021a, February). Crustal fault zones (CFZ) as geothermal power systems: 3D variation of permeability and related processes. In Stanford Geothermal Workshop.

Duwiquet, H., Guillou-Frottier, L., Arbaret, L., Bellanger, M., Guillon, T., & Heap, M. J.: Crustal fault zones (CFZ) as geothermal power systems: A preliminary 3D THM model constrained by a multidisciplinary approach. Geofluids, (2021b), 1-24.

Duwiquet, H., Magri, F., Lopez, S., Guillon, T., Arbaret, L., Bellanger, M., & Guillou-Frottier, L.: Tectonic regime as a control factor for Crustal Fault Zone (CFZ) geothermal reservoir in an amagmatic system: A 3D dynamic numerical modeling approach. Natural Resources Research, 31(6), (2022), 3155-3172.

Duwiquet, H. (2022). Les Zones de Failles Crustales comme systèmes géothermiques électrogènes : Apport des modélisations numériques et confrontation aux systèmes naturels.

Faulds, J., Coolbaugh, M., Bouchot, V., Moek, I., & Oguz, K.: Characterizing structural controls of geothermal reservoirs in the Great Basin, USA, and Western Turkey: developing successful exploration strategies in extended terranes. In World Geothermal Congress 2010 (pp. 11-p).

Faulkner, D. R., Lewis, A. C., & Rutter, E. H. (2003). On the internal structure and mechanics of large strike-slip fault zones: field observations of the Carboneras fault in southeastern Spain. Tectonophysics, 367(3-4), (2003), 235-251.

Famin, V., Philippot, P., Jolivet, L., & Agard, P.: Evolution of hydrothermal regime along a crustal shear zone, Tinos Island, Greece. Tectonics, (2004), 23(5).

Guillou-Frottier, L., Duwiquet, H., Launay, G., Taillefer, A., Roche, V., & Link, G.: On the morphology and amplitude of 2D and 3D thermal anomalies induced by buoyancy-driven flow within and around fault zones. Solid Earth, 11(4), (2020), 1571-1595.

Guillou-Frottier, L., Milesi, G., Roche, V., Duwiquet, H., & Taillefer, A.: Heat flow, thermal anomalies, tectonic regimes and high-temperature geothermal systems in fault zones. Comptes Rendus. Géoscience, 356(S2), (2024),1-33.

Horne, R. N.: Three-dimensional natural convection in a confined porous medium heated from below. Journal of Fluid Mechanics, 92(4), (1979), 751-766.

Huttrer, G. W.: Geothermal Power Generation in the World 2015–2020 update report, Proceedings, World Geothermal Congress, Reykjavik, Iceland, April–October 2021 (2021).

Jolie, E., Scott, S., Faulds, J., Chambefort, I., Axelsson, G., Gutiérrez-Negrín, L. C., ... & Zemedkun, M. T. (2021). Geological controls on geothermal resources for power generation. Nature Reviews Earth & Environment, 2(5), 324-339.

Lapwood, E.: Convection of a fluid in a porous medium. In Mathematical proceedings of the cambridge philosophical society (Vol. 44, No. 4, (1948), pp. 508-521). Cambridge University Press.

Ledingham, P., Cotton, L., & Law, R. (2019). The united downs deep geothermal power project.

Lund, J. W., G. W. Huttrer, G. W., Toth, A. N.: Characteristics and trends in geothermal development and use, 1995 to 2020, Geothermics, Volume 105 (2022), 102522 |

Lun-Tao, T., Ouyang, S., Tai-Rong, G., Ching-Ray, L., Hu, K. H., Chun-Li, L., & Chun-Jao, W.: Insight into the geothermal structure in Chingshui, Ilan, Taiwan. TAO: Terrestrial, Atmospheric and Oceanic Sciences, 19(4), (2008), 4.

López, D. L., & Smith, L.: Fluid flow in fault zones: analysis of the interplay of convective circulation and topographically driven groundwater flow. Water resources research, 31(6), (1995), 1489-1503.

Magri, F., Möller, S., Inbar, N., Möller, P., Raggad, M., Rödiger, T., ... & Siebert, C. (2016). 2D and 3D coexisting modes of thermal convection in fractured hydrothermal systems-Implications for transboundary flow in the Lower Yarmouk Gorge. Marine and Petroleum Geology, 78, (2016), 750-758.

Magri, F., Cacace, M., Fischer, T., Kolditz, O., Wang, W., & Watanabe, N.: Thermal convection of viscous fluids in a faulted system: 3D benchmark for numerical codes. Energy Procedia, 125, (2017), 310-317.

Malkovsky, V. I., & Pek, A. A.: Conditions for the onset of thermal convection of a homogeneous fluid in a vertical fault. Petrology, 5(4), (1997), 381-387.

Malkovsky, V. I., & Magri, F.: Thermal convection of temperature-dependent viscous fluids within three-dimensional faulted geothermal systems: Estimation from linear and numerical analyses. Water Resources Research, 52(4), (2016), 2855-2867.

Moeck, I. S.: Catalog of geothermal play types based on geologic controls. Renewable and Sustainable Energy Reviews, 37, (2014), 867-882.

Ord, A., & Oliver, N. H. S.: Mechanical controls on fluid flow during regional metamorphism: some numerical models. Journal of Metamorphic Geology, 15(3), (1997), 345-359.

Paulillo, A., Cotton, L., Law, R., Striolo, A., & Lettieri, P.: Geothermal energy in the UK: The life-cycle environmental impacts of electricity production from the United Downs Deep Geothermal Power project. Journal of Cleaner Production, 249, (2020), 119410.

Patterson, J. W., Driesner, T., Matthai, S., & Tomlinson, R.: Heat and fluid transport induced by convective fluid circulation within a fracture or fault. Journal of Geophysical Research: Solid Earth, 123(4), (2018), 2658-2673.

Rohit, R. V., Kiplangat, D. C., Veena, R., Jose, R., Pradeepkumar, A. P., & Kumar, K. S.: Tracing the evolution and charting the future of geothermal energy research and development. Renewable and Sustainable Energy Reviews, 184, (2023), 113531.

Rowland, J. V., & Sibson, R. H. (2004). Structural controls on hydrothermal flow in a segmented rift system, Taupo Volcanic Zone, New Zealand. Geofluids, 4(4), (2004) 259-283.

Scibek, J.: Multidisciplinary database of permeability of fault zones and surrounding protolith rocks at world-wide sites. Scientific Data, 7(1),(2020), 95.

Wibberley, C. A., Yielding, G., & Di Toro, G.: Recent advances in the understanding of fault zone internal structure: a review. Geological Society, London, Special Publications, 299(1), (2008), 5-33.

Wisian, K. W., & Blackwell, D. D.: Numerical modeling of Basin and Range geothermal systems. Geothermics, 33(6), (2004), 713-741.

Yang, T., Yang, X., Duan, Q., Chen, J., & Dekkers, M. J.: Rock magnetic expression of fluid infiltration in the Yingxiu-B eichuan fault (Longmen Shan thrust belt, C hina). Geochemistry, Geophysics, Geosystems, 17(3), (2016), 1065-1085.

Zoback, M. D., Barton, C. A., Brudy, M., Castillo, D. A., Finkbeiner, T., Grollimund, B. R., & Wiprut, D. J.: Determination of stress orientation and magnitude in deep wells. International Journal of Rock Mechanics and Mining Sciences, 40(7-8), (2003), 1049-1076.

Zoback, M. L.: First-and second-order patterns of stress in the lithosphere: The World Stress Map Project. Journal of Geophysical Research: Solid Earth, 97(B8), (1992), 11703-11728.